



Potential impacts of 1.5 °C and 2 °C global warming levels on drought modes over Eastern Africa

Mariam Nguvava^{1,2} · Babatunde J. Abiodun²

Received: 14 January 2023 / Accepted: 21 October 2023 / Published online: 23 November 2023
© The Author(s) 2023, corrected publication 2023

Abstract

This study examines the impacts of 1.5 °C and 2.0 °C global warming levels (GWLs) on the characteristics of four major drought modes over Eastern Africa in the future under two climate forcing scenarios (RCP4.5 and RCP8.5). The droughts were quantified using two drought indices: the standardized precipitation evapotranspiration index (SPEI) and the standardized precipitation index (SPI) at 12-month scale. Four major drought modes were identified with the principal component analysis (PCA). Multi-model simulation datasets from the Coordinated Regional Climate Downscaling Experiment (CORDEX) were analysed for the study. The skill of the models to reproduce the spatial distribution and frequency of past drought modes over Eastern Africa was examined by comparing the simulated results with the Climate Research Unit (CRU) observation. The models give realistic simulations of the historical drought modes over the region. The correlation between the simulated and observed spatial pattern of the drought modes is high ($r \geq 0.7$). Over the hotspot of the drought modes, the observed drought frequency is within the simulated values, and the simulations agree with the observation that the frequency of SPI-12 droughts is less than that of SPEI-12 droughts. For both RCP4.5 and RCP8.5 scenarios, the simulation ensemble projects no changes in the spatial structure of the drought modes but suggests an increase in SPEI-12 drought intensity and frequency over the hotspots of the drought modes. The magnitude of the increase, which varies over the drought mode hotspots, is generally higher at 2 °C than at 1.5 °C global warming levels. More than 75% of the simulations agree on these projections. The projections also show that the increase in drought intensity and frequency is more from increased potential evapotranspiration than from reduced precipitation. Hence, the study suggests that to reduce impacts of global warming on future drought, the adaptation activities should focus on reducing evaporative loss surface water.

Keywords Eastern Africa · Drought modes · Simulations · SPEI-12

✉ Mariam Nguvava
mariamnguvava@sua.ac.tz

¹ Department of Geography and Environmental studies, College of Natural and Applied Sciences, Sokoine University of Agriculture, Morogoro, Tanzania

² Climate System Analysis Group, Department of Environmental and Geographical Science, University of Cape Town, Cape Town, South Africa

1 Introduction

Drought is a threat in Eastern Africa because of its socio-economic impacts on agriculture, water resources and the environment (Lyon and DeWitt 2012; Cook and Vizi 2012). Drought induces a wide range of devastating situations in this region. For example, the drought of 1970s over the northeast of Eastern Africa induced more than 300,000 deaths and that of Ethiopia in 1984–1985 led to about 450,000 deaths (Degefu 1987). The widespread drought episode of 1999 affected Kenya, Ethiopia, Burundi, Eritrea, Rwanda and Uganda, causing economic instabilities over these countries (UNDP 2008). In 1998–2005, a persistent drought destroyed crops and livestock and caused a major food shortage in Tanzania (Kijazi and Reason 2009). The 2008–2010 droughts hit most Eastern Africa countries and affected over 8 million people (Muller 2014). Eastern Africa drought of 2010–2011 caused a widespread famine that resulted in humanitarian crises, affecting more than 11 million people (FEWSNET 2011; Robinson et al. 2014). It was the worst drought in the past 60 years over this region (Funk 2011; ACTED 2011). In December 2015, the government of Ethiopia calls for emergency assistance for about 10 million people because of drought caused by seasonal rain failure in the region. The aftereffects of this drought continued for a prolonged period and by 2016 about 22 million people required food relief assistance, and about 2 million people experienced acute malnutrition (Philip et al. 2018). As drought remains a critical problem in Eastern Africa, there is a need for more studies on drought characteristics (e.g., intensity and frequency) over the region. Such studies will provide information for developing reliable mitigation measures against drought.

Studies have reported an increase in the frequency and intensity of droughts in Eastern Africa over the past three decades particularly in Somalia, Ethiopia and Kenya, (e.g. Viste et al. 2013; Shongwe et al. 2011; Damberg and Aghakouchak 2014). Some of these studies have projected that this increase may continue into the future due to global warming (IPCC 2014; Dai 2011; Shongwe et al. 2011; Anyah and Qiu 2010). For example, the analysis of temperature trends of station data that was done by Christy et al. (2008) over Kenya and Tanzania showed a rise in minimum temperature over this region. Omumbo et al. (2011) found a statistically significant upward trend in minimum, maximum and mean temperatures over some parts of Eastern Africa for the past 30 years. These temperature trends will generally accelerate drought condition in the region (Damberg and Aghakouchak 2014). Patricola and Cook (2011) simulated large precipitation reductions at the end of twenty-first century over parts of Eastern Africa. Based on the Coupled Model Intercomparison Project version 3 (CMIP3) models, Anyah and Qiu (2010) projected the high likelihood of increase in extreme warmer minimum and maximum temperatures as well as increase in the number of days with T_{min} and T_{max} greater than 2°C over tropical Eastern Africa. Adhikari et al. (2016) projected a decreased water supply for agriculture in Tanzania especially in dry seasons, under the business-as-usual climate scenario (i.e. RCP 8.5). However, most of these studies have used temperature and/or precipitation to characterize drought. Instead, drought in this region is influenced by both rainfall and evapotranspiration, and various studies (e.g. Cook and Vizi 2012; Nguvava et al. 2019; Abiodun et al. 2019; Abiodun et al. 2021) have shown that global warming may increase evapotranspiration in the future. Hence, there is a need to use a drought index that incorporates both rainfall and potential evapotranspiration to quantify the future impact of climate change on droughts in Eastern Africa.

As part of efforts to minimize impacts of the global warming, the 21st Conference of the Parties to the United Nations Framework Convention on Climate Change (UNFCCC) resolved to limit the increase in global mean average temperature to well below 2 °C above pre-industrial levels, and in fact to pursue efforts to limit the temperature increase to 1.5 °C, because some studies have shown that 2 °C above pre-industrial levels is inadequately safe (UNFCCC 2015). Peters et al. (2013) highlighted that with the continuing emissions of carbon dioxide that follows the high end emission scenarios, it may be more difficult to limit global warming below 2 °C. To limit the warming below 2 °C, immediate, significant and sustained global mitigations are required. However, understanding the differences in regional impacts of 1.5 °C and 2 °C global warming is essential and has been the topic of investigation by several studies. For example, James and Washington (2013) reported larger precipitation anomalies observed at 2 °C over continental Africa, and these anomalies found to be strengthened and extended at higher warming levels, i.e. 3 °C and 4 °C. King et al. (2017) reported that limiting warming to 1.5 °C relative to 2 °C would reduce the frequency of extreme heat events and heat in the Coral Sea region off the Australian coast by 26% and 22% respectively. Su et al. (2017) documented a lower evapotranspiration rate for 1.5 °C relative to warming of 2 °C over the Tarim River Basin, China. They furthermore projected that regional warming of 1.5 °C would occur later than the global average, whereas regional warming of 2 °C would occur earlier than the global average. Ying et al. (2017) found that relative to the pre-industrial era, the mean temperature over Asia would increase by 2.3 °C and 3.0 °C, at global warming targets of 1.5 °C and 2 °C respectively. However, only few studies have reported the impacts of the various global warming levels (GWLs) on the Eastern Africa climate (e.g. Osima et al. 2018; Nguvava et al. 2019). Most future projection studies have focused on specific time period using certain emission scenario (e.g. Otieno and Anyah 2013; Niang et al. 2014; Adhikari et al. 2016). Therefore, the current study analysed drought projections using the various GWLs at certain emission scenarios.

Future climate change projections are usually based on Global Climate Model (GCMs) simulations (e.g. Wang et al. 2017; Ying et al. 2017). But, due to their low horizontal grid resolutions, these simulations do not resolve well the influence of local forcings (like terrain and vegetation effects, and land-sea contrasts) that modulate the climate signal at finer scales (Rummukainen 2010). Downscaling GCM simulations with regional climate models (RCMs) accounts for some of the processes not resolved by GCMs. For instance, Su et al. (2017) used regional model COSMO-CLM a downscale of GCM ECHAM6 to project potential evapotranspiration rates under global warming scenarios 1.5 °C and 2 °C in China. However, robust climate change projections require a multi-RCM downscaling of multi-GCM simulations. This has been a big challenge for many institutions in Africa because of the associated computational cost. To address the challenge, the Coordinated Regional Climate Downscaling Experiment (CORDEX; Giorgi et al. 2009; Giorgi and Gutowski 2015) has provided a multi-RCM downscaling of some GCMs and made the data available publicly. Despite this, only few studies have utilized the CORDEX data impact of climate change on Eastern Africa climate (e.g. Souverijns et al. 2016; Endris et al. 2013); meanwhile, there is dearth of information on future projection of drought under the 1.5 °C and 2 °C warming above the pre-industrial level.

Hence, the aim of this study is to utilize the CORDEX datasets in examining the influence of 1.5 °C and 2 °C warming on drought in Eastern Africa under two future climate scenarios (RCP4.5 and RCP8.5). Section 2 of this paper describes the datasets and methods used in analysing them. Section 3 presents and discusses the results of the analysis while Section 4 gives the conclusion remarks.

2 Methodology

2.1 The study domain

Eastern Africa region consists of eight developing countries (i.e. Tanzania, Ethiopia, Somalia, Kenya, Uganda, Djibouti, Burundi, Rwanda, and South Sudan) located in the easterly part of sub-Saharan Africa (Fig. 1). In this study, we have defined the region as the area lying within 28 °E and 52 °E longitudes and 12 °S and 12 °N latitudes. The region generally has a semi-arid climate and experiences small variations in temperature throughout the year, but exhibits a high degree of spatiotemporal variability in rainfall (Yang et al. 2015). Eastern Africa is characterized by two major rainfall regimes: the bimodal regime rains in March–May (MAM) and October–December (OND) and the unimodal regime rains in June–September (JJAS) and December–March (DJFM) (Nicholson 2017; Yang et al. 2015).

2.2 Data and methods

Observation and simulation datasets (i.e. monthly total precipitation, maximum, minimum and mean temperature) were analysed for the study. The observed datasets were extracted from the Climate Research Unit (CRU v.3.22; Harris et al. 2014) of the University of East Anglia, UK. The CRU datasets are gridded ($0.5^\circ \times 0.5^\circ$ global grid resolution) compiled from meteorological station data over the period 1901–2014 (Harris et al. 2014). These data were downloaded from <http://badc.nerc.ac.uk/data/cru/>. The model simulation datasets were the outputs of 20 CORDEX RCMs forced by CMIP5 GCMs over CORDEX Africa region (CORDEX data archive: <http://cordex.dmi.dk/joomla>). The RCM-GCM matrix is shown in Table 1. The period from 1971 to 2001 was used to calculate

Fig. 1 Topography of Eastern Africa

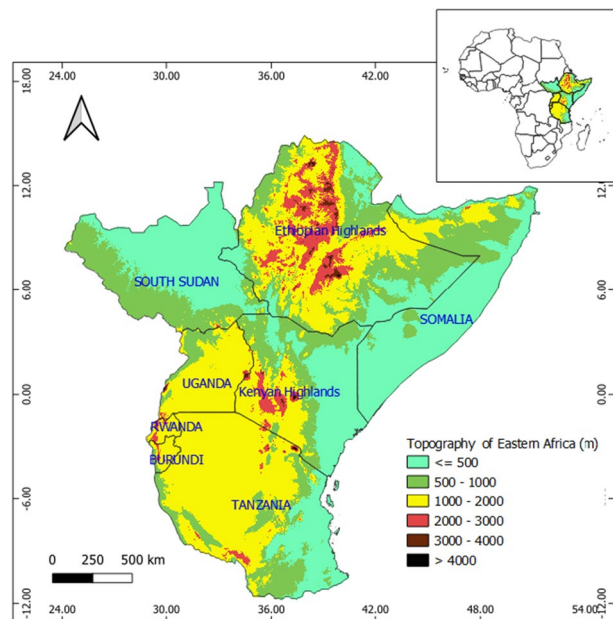


Table 1 Regional climate models and the corresponding CMIP5 global climate models downscaled

CORDEX RCMs	Driving GCMs (CIMAP5)	RCP4.5		RCP8.5	
		1.5 °C	2 °C	1.5 °C	2 °C
SMHI-RCA4	ICHEC_EC_EARTH	2010–2039	2031–2060	2005–2034	2021–2050
	CanESM2	2002–2031	2017–2046	1999–2028	2012–2041
	CNRM-CM5	2021–2050	2042–2071	2015–2044	2029–2058
	CSIRO-Mk3.6	2020–2049	2033–2062	2018–2047	2030–2059
	HadGEM2-ES	2016–2045	2032–2061	2010–2039	2023–2052
	IPSL-CM5A-LR	2002–2031	2020–2049	2002–2031	2016–2045
	MIROC-MIROC5	2026–2055	2059–2088	2019–2048	2034–2063
	MPI-ESM-LR	2006–2035	2029–2058	2004–2033	2021–2050
	NorESM1-M	2027–2056	2062–2091	2019–2048	2034–2063
DMI-HIRHAM5	NorESM-M	2027–2056	2062–2091	2019–2048	2034–2063
CLMcom-CCLM4-8-17	ICHEC_EC_EARTH	2010–2039	2031–2060	2005–2034	2021–2050
	MPI-ESM-LR	2006–2035	2029–2058	2004–2033	2021–2050
	HadGEM2-ES	2016–2045	2032–2061	2010–2039	2023–2052
	CNRM-CM5	2021–2050	2042–2071	2015–2044	2029–2058
CNRM-ALADIN52	CNRM-CM5	2021–2050	2042–2071	2015–2044	2029–2058
BCCR-WRF331	NorESM-M	2027–2056	2062–2091	2019–2048	2034–2063
KNMI-RACMO22E	ICHEC	2006–2035	2028–2057	2003–2032	2021–2050
	HadGEM2-ES	2016–2045	2032–2061	2010–2039	2023–2052

the historical drought of model simulations and compare with gridded observation. The projected change in drought for 1.5 °C and 2 °C global warming were analysed using the 30-year period the GCM simulation reaches 1.5 °C and 2 °C warming for both RCP 4.5 and RCP8.5. Details of how the 30-year periods of 1.5 °C and 2 °C warming level were calculated can be obtained from Vautard et al. (2014). The impact of these warming levels was determined by comparing the simulation with those of reference period (1971–2000). This reference period “1971–2000” was chosen because it is the most commonly used control period in climate impact application studies and in several previous research on GWL over Africa (e.g. Nikulin et al. 2018; Osima et al. 2018; Pinto et al. 2018). Therefore, it is used here to ensure that the results of the present study are consistent with other previous studies. In addition, using a climatological period starting beyond 1971 might cause the results to overlap with the GWL climatological projections. All simulations dataset were regridded to $0.5^\circ \times 0.5^\circ$.

The standardized precipitation evapotranspiration index (SPEI; Vicente-Serrano et al. 2010; Beguería et. 2014) was used to quantify drought on this study. SPEI characterize droughts based on climate water balance i.e. precipitation (P) minus potential evaporation (PET). Estimation of PET will be done using Hargreaves (Hg) equation (Hargreaves and Samani 1985). The Hg equation requires daily maximum and minimum temperatures (TMAX and TMIN), monthly mean precipitation and the latitudinal position of the site. Other popular PET methods are available. These include Thornthwaite (Th; Thornthwaite 1948) and Penman–Monteith (PM; (Monteith 1965; Penman 1948)) equations. Th computation only requires mean daily temperature and latitudinal position of the site, but has some drawbacks. Among the deficiencies is that the Th equation underestimates PET in tropical and humid equatorial regions. PM is a more physically based method for calculation of PET, but the method is highly demanding in terms of data (e.g. wind speed,

relative humidity and solar radiation). Unfortunately, these datasets are not readily available in the study domain. Beguería et al. (2014) showed that the use of the Hg method is the best option especially over regions with limited data. To understand the range of drought intensity, SPEI values are categorized according to classes (Mavromatis 2007). Normal conditions are established from the aggregations of two classes: $-1 < \text{indices} < 0$ (mild drought) and $0 < \text{indices} < 1$ (slightly wet). The values are positive or negative for greater or less than mean precipitation, respectively. The more negative the value for a given location, the more severe the drought. In the present study, SPEI is used to characterize 12-month droughts, which impact both agriculture and surface hydrological systems especially reservoirs and streams. The period 1971–2000 was used as the reference period for calculating the SPEI-12 and SPI-12 for the historical and future climates.

The principal component analysis (PCA; Jolliffe 2002) was used to obtain drought modes over the study domain. The PCA is a multivariate variable-reduction procedure commonly used in climate research for defining the leading spatial and temporal patterns of climate variability (Richman 1986). For the PCA, we calculated the covariance matrix from standardised normalised variables, calculated the matrix's eigenvectors and eigenvalues and ordered the eigenvectors according to the magnitude of eigenvalues. The eigenvector with the highest eigenvalue represents the first principal factor and the mode with the largest variability in the dataset. PCA has been used for the regionalization of drought at different spatial and temporal scales (e.g. Santos et al. 2010; Indeje and Semazzi 2000; Ujeneza and Abiodun 2015). Here, we applied PCA with a varimax rotated option, because previous studies (e.g. Jolliffe 2002) showed that varimax rotation enhances the physical application and understanding of PCA results. The PCA was applied to the SPEI-12 and SPI-12 of each dataset (observations and RCM simulations), and the first four principal factors of the PCA were retained as the most significant drought modes (DM1, DM2, DM3 and DM4) in the dataset.

3 Results and discussion

3.1 Observed and simulated drought modes in historical climate

To assess the credibility of CORDEX RCMs in simulating historical drought modes over Eastern Africa, the characteristic of the simulated drought modes in historical climate is compared with the observed (Figs. 2 and 3). The RCM ensemble replicates the spatial pattern of the observed drought modes well (Fig. 2). For all the drought modes, the correlation between the simulated and observed pattern is high ($r \geq 0.7$). The model ensemble mean features the core hotspot of the modes (depicted by red boxes) at location as in observation. The first drought mode (DM1) explains about 21% (CRU) and 13% (model ensembles mean) of the drought variability and features its highest positive loadings (≈ 0.8) over northeast Kenya and south Somalia and a negative loading (≈ 0.6) over north Sudan and northwestern Ethiopia. The second drought mode (DM2) explains 12% (CRU) and 14% (ensembles mean) of the SPEI-12 variance and features its highest positive loadings (≈ 0.6) over Tanzania. DM2 highest negative loadings (≈ 0.2) are located far north of Eastern Africa. Drought mode (DM3) explains 11% and 16% of CRU and ensemble mean respectively of the SPEI-12 variance and shows its highest positive loadings (≈ 0.6) over the horn of Africa (i.e. north Somalia and east Ethiopia). The last drought mode for this work (DM4) accounts for 11% (CRU) and 15% (ensembles mean) of the variability and features

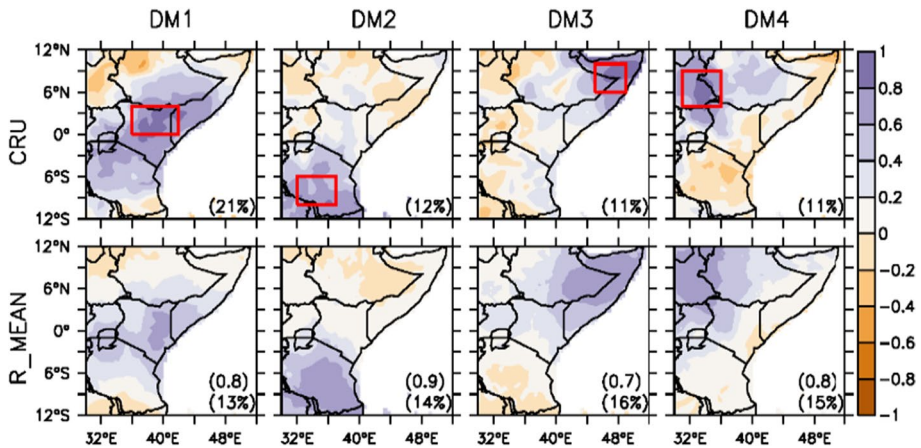


Fig. 2 The observed and simulated (ensembles mean) loadings of 12-month SPEI over Eastern Africa for the period 1971–2000. The percentage of variance explained on each mode (DM1, DM2, DM3 and DM4) of CRU, and each ensemble is indicated in the lower right corner of each panel. The spatial correlation between observed and simulated loadings for each mode is shown above each variance. The red boxes represent the core hotspots (positive loadings) of the drought modes

its highest positive loading over most parts of South Sudan and some parts of west-central Ethiopia and negative loadings along the Eastern Africa coastal area.

In general, these drought modes correspond to different rainfall climate zones in Eastern Africa (Cook and Vizy 2012; Lyon 2014; Yang et al. 2015). DM1 area has bimodal rainfall climatology with peaks during MAM (heavy rains) and OND (light rains). According to Yang et al. (2015), DM4 area has similar pattern of rainfall climatology as DM1 area, and therefore, the differences can be on the large scale systems (Teleconnections) that influence their climate. For instance, DM4 region is affected strongly by the Somali jet (Findlater 1977; Segele et al. 2009) and Asian monsoon (Camberlin 1997; Vizy and Cook 2003), and relatively, no effect occurs to DM1 region. DM2 and DM3 have both unimodal rainfall climatology and with similarities in their intensity ranges at peak season but differs in the time of season. While DM2 peaks in DJFM, DM3 peaks in JJAS.

The capability of RCMs to reproduce the spatial pattern of the drought modes varies among the simulations (Fig. 3a and b). For all drought modes, the correlation between individual simulation and the observation varies between 0.3 and 0.9. All the simulations show their best performance in simulating DM2 ($r = 0.6 \leq r \leq 0.9$) and their worst performance in simulating DM3 ($r = 0.3 \leq r \leq 0.8$). The majority of the models (95%) correlations were above 0.7 in DM2 and in DM3, and majority of the models (80%) correlations were below 0.6. The best performance of the model in simulating DM2 may be that the modes are mostly controlled by the large-scale atmospheric circulation or teleconnections (e.g. ENSO and IOD) that are well reproduced by the forcing GCM simulations. Several studies have shown DM2 hotspot to have high correlation with tropical Pacific Ocean and western Indian Ocean (e.g. Trenberth et al. 2014; Nicholson 1996; Tierney et al. 2013; Dutra et al. 2013; Lott et al. 2013). As for DM4, Lyon (2014) and Segele et al. (2009) have reported that the hotspot is mostly linked with tropical Atlantic Ocean but also local processes have some impacts. The recent analysis by Nguvava (2020) has shown that the DM1 region is linked with several teleconnections including IOD, ENSO as well as Tropical Atlantic Ocean. Having such diversity could also be the reason for the climate models to have weak

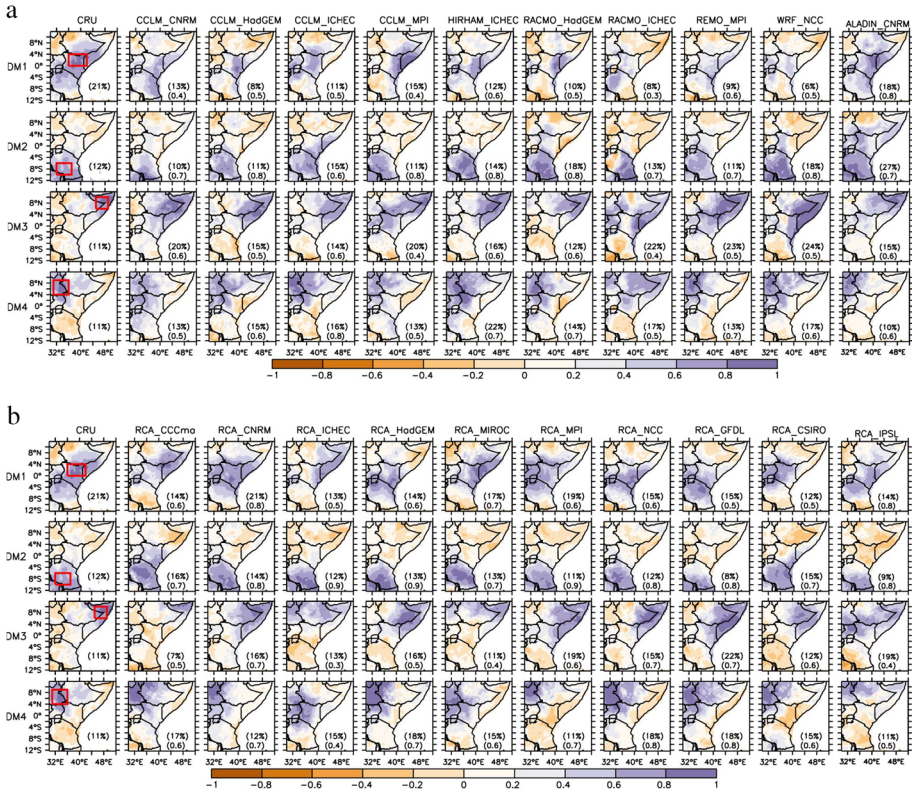
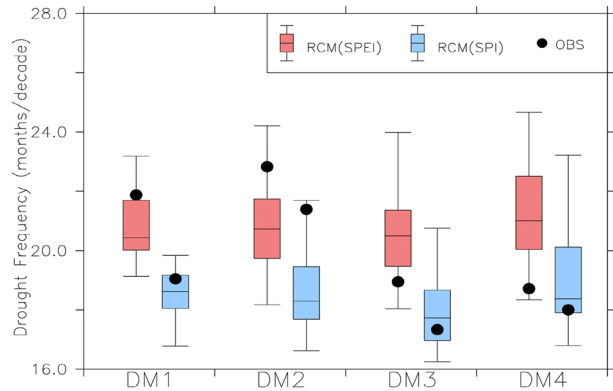


Fig. 3 **a** The observed and simulated loadings of the 12-month SPEI over Eastern Africa for the period 1971–2000. The percentage of variance explained by the CRU and each RCM model for all drought modes is indicated in the lower right corner of each panel. The spatial correlation between the observed and the simulated loadings is shown beneath each variance. **b** The same as Fig. 3a but for other RCMs

identification of this drought mode. Another interesting observation is that every model has produced the pattern as of CRU although not in the same order. For example, CCLM-CNRM, CCLM-MPI, RACMO-ICHEC, REMO-MPI and WRF-NCC (Fig. 3a) all show drought mode 3 with highest variance than other modes, and therefore, this is a leading mode for these models. Among the RCMs analyzed, RACMO-ICHEC shows very low correlation of drought modes with CRU especially for DM1 ($r = 0.3$). This describes that RACMO-ICHEC identifies only a small part of DM1 positive loading that CRU observed. Similar results can be seen for RCA-ICHEC but for DM3 (Fig. 3b). Based on these observations, the global model ICHEC that was downscaled with different RCMs seems to carry the weakness of not being able to capture properly the global patterns that control drought over the most part of Eastern Africa except for DM2 region which has the highest correlation in both RACMO-ICHEC ($r = 0.7$) and RCA-ICHEC

The RCMs give generally weak simulations of drought frequency over the core hotspot of the DM1, DM2, DM3 and DM4 (Fig. 4). The models have either underestimated or overestimated the drought frequency. For example, for DM2, simulations have generally underestimated drought frequency because less than 25% of the simulation lies in the quartile the observation is in, and more than 75% of the simulation produces results below the

Fig. 4 The frequency of 12-month droughts ($\text{SPEI} \leq -1$; $\text{SPI} \leq -1$) over the core area of the four drought modes (DMs: DM1, DM2, DM3 and DM4) in the historical climate (1971–2000), as depicted by CRU observation and RCM simulations. The boxplots represent the interquartile model ensemble spread range: minimum, 1st quartile, median, 3rd quartile and maximum values



observed value. As for DM4, simulations generally overestimated the drought frequency as they produce frequency above the observed value, i.e. the observed frequency found below the first quartile of the model simulations. However, for all the DMs, the observed drought frequency (SPEI -12 and SPI -12) falls within the simulations spread. Also, for all the drought modes, the drought frequency of DM1 is best simulated by the models for both SPEI -12 and SPI -12 indices while DM2 drought frequency was poorly simulated for all the drought indices. In addition, the performance of the simulations at reproducing the drought frequency is generally better with SPI -12 than with SPEI -12 (especially for DM1, DM3 and DM4). For instance, in DM1, more than 75% of the simulations overestimate the SPEI -12 drought frequency, but less than 75% of them overestimate the SPI -12 drought frequency. Also, in DM3 and DM4, while the observed SPI -12 drought frequency is within the first and third quartiles of the simulated values, the observed SPEI -12 drought frequency is below the first quartile. The better performance of the RCMs in simulating SPI -12 than SPEI -12 suggests a larger bias in the simulated PET than in the simulated precipitation in Eastern Africa region. Nevertheless, for all DMs, the observation and the simulations agree that SPEI -12 droughts are more frequent than the SPI -12 droughts. The difference ranges from ~ 3 months/decade (CRU) and ~ 2 months/decade (RCM median) in DM1 to ~ 0.5 month's decade⁻¹ (CRU) and ~ 3 months decade⁻¹ (RCM median) in DM4. This suggests that the inclusion of the PET enhances the intensity and frequency of the droughts over the hotspots. The results agree with Vicente-Serrano et al. (2010, 2012) that SPI may underestimate drought severity and frequency.

3.2 Impacts 1.5 °C and 2 °C warming on drought modes under RCP4.5 and 8.5 scenarios

The simulation ensemble mean projects no changes in the spatial structure of the drought modes under both 1.5 °C and 2.0 °C global warming (Figs. 5 and 6). The correlation between the spatial distribution of the drought modes in past and future climate is very strong ($r = 0.9 < r < 1$), the location of drought mode cores remains the same, and the changes in the percentage of variance of explained by each drought mode are very small ($< 2\%$). This suggests that the global warming may not alter the location and structure of these major drought patterns. The weak sensitivity of the structure of the drought modes to the global warming may be attributed and may be because the location of the large-scale drivers (e.g. ENSO, IOD) has been projected not to change with the global warming.

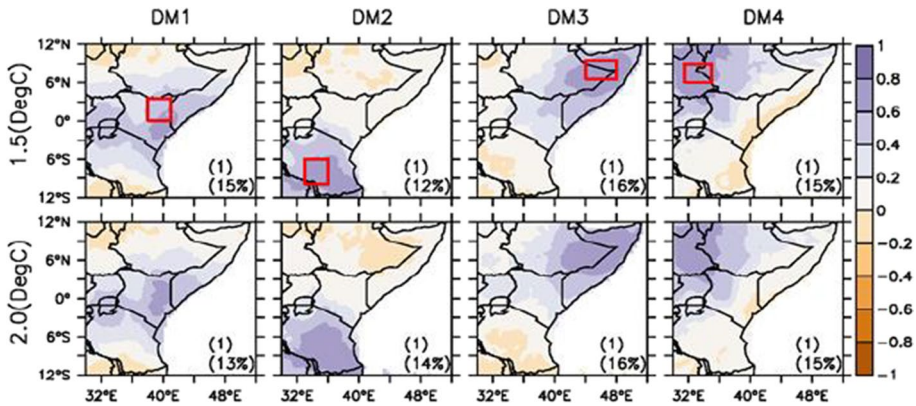


Fig. 5 The projected spatial structure of the 12-month SPEI over Eastern Africa for the future climate, given 1.5 °C and 2.0 °C global warming levels under RCP4.5 scenarios. The percentage of variance explained by each drought mode is indicated in the lower right corner of each panel. The spatial correlation between the historical and future simulation loadings for each mode is shown above the variance

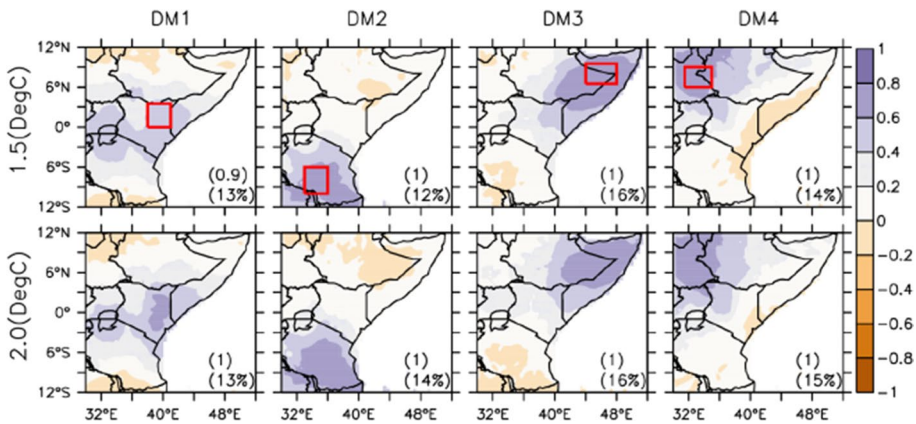


Fig. 6 The same as Fig. 5 but for RCP 8.5

For example, Vecchi and Wittenberg (2010) found no clear evidence of ENSO activity to increase or decrease when considering future global warming trends, and Stevenson et al. (2011) indicated insignificant weakening of ENSO variability with higher CO₂ concentrations. Cai et al. (2013) also documented a non-change of the IOD mean frequency with global warming levels but only a minor change of an amplitude reduction between positive and negative dipole events.

The RCMs project a substantial increase in the intensity and frequency of SPEI-12 droughts over DM1, DM2, DM3 and DM4 hotspots under both 1.5 °C and 2 °C global warming (Fig. 7). The magnitude of the increase, which is generally higher under 2 °C than 1.5 °C warming, varies over the DM cores. The highest increase in SPEI-12 drought intensity (i.e. reduced SPEI-12: – 0.4 and – 0.6 for 1.5 °C and 2 °C warming, respectively) and frequency (about 15 and 20 months per decade⁻¹ for 1.5 °C and 2 °C warming, respectively) occurs over DM4 hotspot, while the least increase in the intensity (i.e. reduced

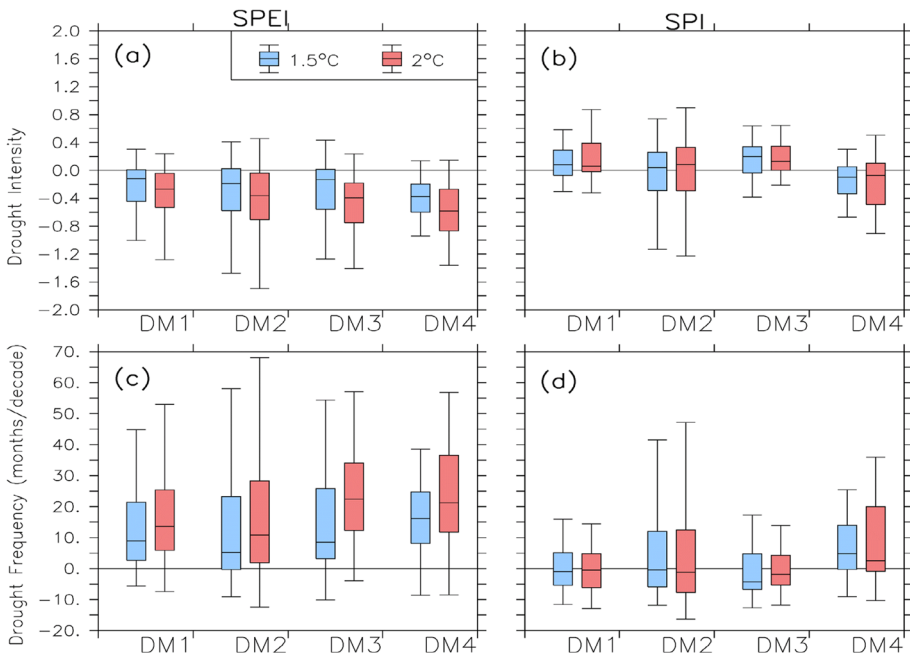


Fig. 7 Projected changes with regard to the intensity (a, b) and the frequency (c, d) of 12-month droughts (SPEI < - 1; 12-month SPI < - 1) under a future climate, at 1.5 °C and 2.0 °C global warming levels under the RCP4.5 scenario. The changes are calculated with respect to the historical climate (1971–2000). The boxplot shows the interquartile of the simulation spread: minimum, 1st quartile, median, 3rd quartile and maximum values

SPEI-12: - 0.1 and - 0.3 for 1.5 °C and 2 °C warming respectively) and frequency (about 10 and 12 months per decade⁻¹ for 1.5 °C and 2 °C warming, respectively) occurs over DM1 hotspot. But, the largest difference between the impacts of the two warming levels is over DM3. However, there are some discrepancies among the simulations on the sign and magnitude of the projected changes. For example, in the 2 °C warming projection over the DM4 (Fig 7a and c), the projected changes in the drought intensity vary from - 1.6 to + 0.4, and the changes in drought frequency vary from - 10 to 70 months decade⁻¹. Nevertheless, more than 75% of the simulations agree on the both 1.5 °C and 2 °C warming will increase drought intensity and frequency over the four drought hotspots. This result agrees with previous studies that project a decrease in precipitation and an increase potential evapotranspiration over most parts of Eastern Africa (e.g. Cook and Vizy 2012). However, the use of SPEI-12 in the present study combines the projected changes in precipitation and evapotranspiration in accessing impacts of the global warming on droughts.

The projected changes in SPI-12 drought differ from that of SPEI-12 in many aspects (Fig. 7). For example, over three of the DMs (DM1, DM2 and DM3), the projected changes (ensemble mean) in SPI drought characteristics have opposite sign to that of SPEI-12. In contrast to SPEI-12 results, an increase in SPI-12 (wet condition) and a decrease in SPI-12 drought frequency are projected over the three DM hotspots (DM1, DM2 and DM3). Under the 1.5 °C warming level, the maximum increase in SPI (about + 0.2) and the maximum decrease in drought frequency occur over the DM3. In addition, over DM1 hotspot, where the signs of changes in SPI-12 and SPEI-12 drought are the same, the magnitude of

the changes (for both drought intensity and frequency) is smaller in SPI-12 than SPEI-12. Under 2 °C warming, the simulation ensemble projects a decrease of about -0.1 in SPI-12 drought intensity (compared to about -0.6 in SPEI-12) with the simulation spread ranging between -0.6 and $+0.4$ (compared -1.4 and 0.2 in SPEI-12). The corresponding increase in SPI-12 drought frequency (ensemble mean) is about 3 months decade⁻¹ (compared to 20 months per decade⁻¹ in SPEI-12). Furthermore, the level of agreement among the simulations on the projections is weaker in SPI-12 (less than 75% of the simulations agree) than in SPEI-12 (more than 75% of the simulations agree). The differences in SPI-12 and SPEI-12 projection are due the influence of potential evapotranspiration on droughts. While the SPEI-12 projection accounts for this influence, SPI-12 projections do not. It is expected that the global warming would enhance potential evapotranspiration, and hence induce a drier climate over Eastern Africa. However, the difference between the SPEI-12 and SPI-12 projection stresses the need to include potential evapotranspiration in projecting impact of global warming on droughts over the region.

The RCP8.5 projection features similar drought characteristics as in RCP4.5 projection (Fig. 8). The spatial distribution of the droughts modes is the same with that in historical and RCP4.5 patterns. This further suggests that the spatial structure distribution of major drought modes over the Eastern Africa may be invariant to the global warming levels or climate forcing scenarios. While the changes in the drought frequency and drought intensity are sensitive to the warming levels (1.5 °C and 2.0 °C), they do not vary much with the climate forcing scenarios (1.5 °C and 2.0 °C). For instance, with 2 °C warming, the difference between RCP4.5 and RCP8.5 projections (i.e. ensemble mean) is small over DM4; for drought intensity, it is less than 0.2; and for drought frequency, it is less than 5 months decade⁻¹. The simulation spread in the two is also comparable, although the level of agreement is somehow weaker in RCP8.5 projection, where less than 75% of the simulations

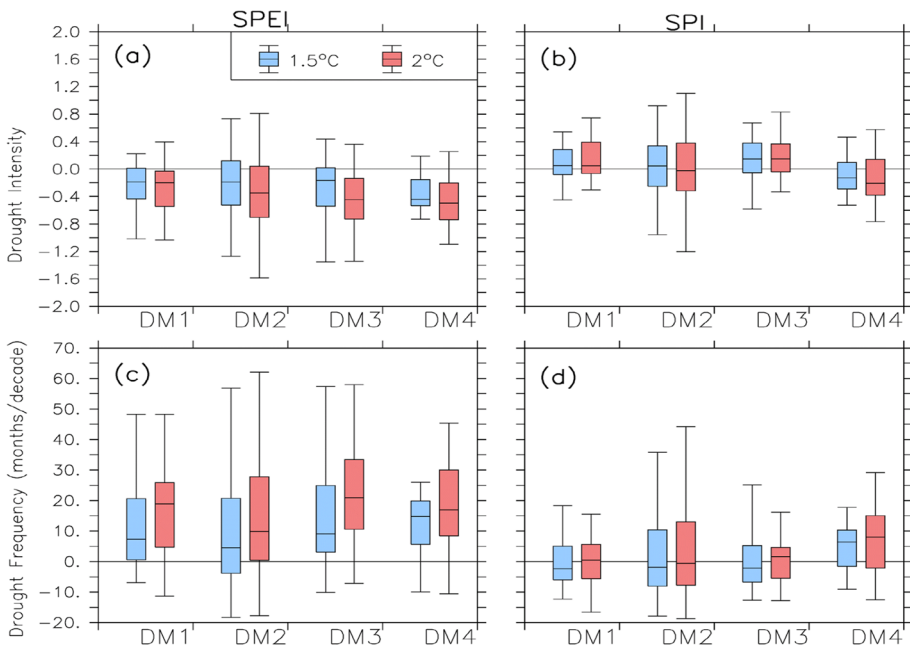


Fig. 8 The same as Fig. 7 but for RCP 8.5

agree on projected changes over DM2. The discrepancy between SPEI and SPI results also features RCP8.5 projection, in wetter condition, and less frequent SPI droughts are also projected over the DMs hotspots except over DM4. Hence, at a given warming level, there is no difference in the Eastern African drought characteristics under RCP4.5 and RCP8.5. Some studies have reported a similar result for different variables over some region (Chen et al. 2017; Karmalkar and Bradley 2017). For example, Chen et al. (2017) found no significant difference in projected mean temperature and temperature extremes over China under RCP4.5 and RCP8.5 at both 1.5 °C and 2.0 °C warming levels.

However, the most robust information from the RCP4.5 and RCP8.5 projections is that the spatial structure of the major drought modes in Eastern Africa may not change with the global warming levels (1.5 °C and 2 °C), but the intensity and frequency of SPEI-12 drought over DM1, DM2, DM3 and DM4 hotspots may increase with the warming levels, while the projected change of SPI droughts may not change substantially. This suggests that the impact of the global warming on future drought may be stronger through increased potential evapotranspiration than through decreased precipitation. Hence, future drought mitigation options over the DM1, DM2, DM3 and DM4 hotspots should focus more on activities that minimize loss of soil moisture, decrease of water in surface reservoirs and decrease of surface runoff through evaporation. Such activities could include planting of trees and shrubs to protect the land from direct evaporation and lower the strength of wind that accelerates the humidity loss above the surface of water reservoirs (Ritchie 1983). Alvarez et al. (2006) recommended the use of shade structures which reduce the energy available for evaporation and reduce the strength of wind blowing over the water surface specifically for small reserves. For a large dam, Craig et al. (2007) proposed the construction of deeper storages with smaller surface area or dividing the dam into smaller sections to lower the wind flow.

4 Conclusion

This study has examined the potential impacts of on-going global warming on the characteristics of major drought modes in Eastern Africa at 1.5 °C and 2 °C warming levels under RCP4.5 and 8.5 scenarios. The CRU observation and 20 CORDEX RCM simulation datasets were analysed for the study. The simulation datasets consist of rainfall and temperature (maximum and minimum) data for the historical climate (1971–2000) and for the future climate with 1.5 °C and 2 °C warming level under RCP4.5 and 8.5 climate forcing scenarios. The SPEI (a drought index that is based on climate water balance) was used to quantify drought, and the PCA was applied on the SPEI-12 data to obtain the most dominant four drought modes over the region. The characteristics of drought mode considered include the spatial of structure of the drought modes, as well as the intensity and frequency of drought over the hotspots of the drought modes. The capability of the CORDEX simulations to reproduce these characteristics was examined before analysing the simulations to investigate the impacts of the global warming on the drought modes. The results of the study can be summarized as follow:

- The RCM ensemble mean gives a realistic simulation of the characteristics of the four major drought modes over the Eastern Africa. The correlation between the simulated and observed drought spatial structure is high ($r > 0.7$), and the observed drought frequency over the drought mode hotspots falls within simulation spread.

- The simulations and CRU observation agree that using SPI (instead of SPEI) produced a lower drought frequency in the historical climate. However, the RCMs perform better at simulating SPEI than at reproducing SPI.
- The RCM ensemble projects that the location and spatial structure of the drought modes are invariant to the global warming levels (1.5 °C and 2.0 °C) and to changes in the RCP scenarios (RCP4.5 and RCP8.5). Nevertheless, the increases in the warming levels are projected to substantially increase in the intensity and frequency of SPEI-12 drought over the core of the drought modes.
- The SPI-12 projections (i.e. changes in drought intensity and frequency) give an opposite result to that of SPEI-12 over the core of the drought modes, and the magnitude of SPI-12 changes is smaller than that of SPEI-12 over the four drought modes.

Future work can improve the robustness of these results in many ways. For example, this present work has focused on droughts by using SPEI and SPI indices. Following Vicente-Serrano et al. (2010), the SPEI was calculated using potential evapotranspiration, which is only equal to actual evaporation when there is sufficient surface water supply. The SPEI might have overestimated the drought intensity under the natural condition while SPI might have underestimated it. Hence, using actual evaporation (which is not available for all CORDEX simulation) might improve the quality of the SPEI. Future studies can also extend the study to impact other global warming on agricultural, hydrological and economical droughts by using appropriate drought indices to identify the agricultural, hydrological and economical drought modes. These drought modes might be the same or different from the drought modes identified here, but understanding how the global warming might impact the hotspots of different types of drought will help the policymakers in using most appropriate options in mitigating the impacts. However, the present study has shown that while the global warming may not alter the hotspot of the major drought modes over Eastern Africa, it may increase the intensity and frequency of drought over the hotspot.

Author contributions All authors contributed equally the manuscript preparation

Funding Open access funding provided by University of Cape Town.

Data availability This work uses climate data that are available in the repositories specified in the methodology section.

Declarations

Competing interests The authors declare no competing interests.

Open Access This article is licensed under a Creative Commons Attribution 4.0 International License, which permits use, sharing, adaptation, distribution and reproduction in any medium or format, as long as you give appropriate credit to the original author(s) and the source, provide a link to the Creative Commons licence, and indicate if changes were made. The images or other third party material in this article are included in the article's Creative Commons licence, unless indicated otherwise in a credit line to the material. If material is not included in the article's Creative Commons licence and your intended use is not permitted by statutory regulation or exceeds the permitted use, you will need to obtain permission directly from the copyright holder. To view a copy of this licence, visit <http://creativecommons.org/licenses/by/4.0/>.

References

- Abiodun BJ, Makhanya N, Petja B, Abatan AA, Oguntunde PG (2019) Future projection of droughts over major river basins in Southern Africa at specific global warming levels. *Theor Appl Climatol* 137(3–4):1785–1799. <https://doi.org/10.1007/s00704-018-2693-0>
- Abiodun BJ, Odoulami RC, Sawadogo W, Oloniyo OA, Abatan AA, New M, Lennard C, Izidine P, Egbebiyi TS, MacMartin DG (2021) Potential impacts of stratospheric aerosol injection on drought risk managements over major river basins in Africa Abstract. *Clim Change* 169(3–4). <https://doi.org/10.1007/s10584-021-03268-w>
- ACTED (2011) Horn of Africa. Drought predictable and predicted. Agency for Technical Cooperation and Development, Paris, France
- Adhikari U, Nejadhashemi AP, Herman MR, Messina JP (2016) Multiscale assessment of the impacts of climate change on water resources in Tanzania. *J Hydrol Eng* 22(2):05016034
- Alvarez VM, Baille A, Martínez JM, González-Real MM (2006) Efficiency of shading materials in reducing evaporation from free water surfaces. *Agric Water Manag* 84(3):229–239
- Anyah RO, Qiu W (2010) Characteristic 20th and 21st century precipitation and temperature patterns and changes over the Greater Horn of Africa. *Int J Climatol* 32(3):347–363
- Beguera S, Vicente-Serrano SM, Reig F, Latorre B (2014) Standardized precipitation evapotranspiration index (SPEI) revisited: parameter fitting, evapotranspiration models, tools, datasets and drought monitoring. *Int J Climatol* 34(10):3001–3023
- Cai W, Zheng XT, Weller E, Collins M, Cowan T, Lengaigne M, Yu W, Yamagata T (2013) Projected response of the Indian Ocean Dipole to greenhouse warming. *Nat Geosci* 6(12):999–1007
- Camberlin P (1997) Rainfall anomalies in the source region of the Nile and their connection with the Indian summer monsoon. *J Clim* 10(6):1380–1392
- Chen SHI, Zhi-Hong JIANG, Wei-Lin CHEN, Li L (2017) Changes in temperature extremes over China under 1.5° C and 2° C global warming targets. *Advances in Climate Change Research*
- Christy JR, Norris WB, McNider RT (2008) Surface temperature variations in East Africa and possible causes. *J Clim* 22(12):3342–3356
- Cook KH, Vizy EK (2012) Impact of climate change on mid-twenty-first century growing seasons in Africa. *Clim Dyn* 39(12):2937–2955
- Craig I, Aravinthan V, Baillie C, Beswick A, Barnes G, Bradbury R, Connell L, Cooper P, Fellows C, Fitzmaurice L, Foley J (2007) Evaporation, seepage and water quality management in storage dams: a review of research methods. *Environ Health* 7(3):84–97
- Dai A (2011) Drought under global warming: a review. *Wiley Interdiscip Rev Clim Chang* 2(1):45–65
- Damberg L, AghaKouchak A (2014) Global trends and patterns of drought from space. *Theor Appl Climatol* 117(3–4):441–448
- Degefu W (1987) Some aspects of meteorological drought in Ethiopia. *Drought and hunger in Africa: Denying famine a future*. pp 23–36
- Dutra E, Magnusson L, Wetterhall F, Cloke HL, Balsamo G, Bousssetta S, Pappenberger F (2013) The 2010–2011 drought in the Horn of Africa in ECMWF reanalysis and seasonal forecast products. *Int J Climatol* 33(7):1720–1729
- Endris HS, Omondi P, Jain S, Lennard C, Hewitson B, Chang’a L, Awange JL, Dosio A, Ketiemi P, Nikulin G, Panitz HJ (2013) Assessment of the performance of CORDEX regional climate models in simulating East African rainfall. *J Clim* 26(21):8453–8475
- Famine Early Warning System Network. (2011) East Africa: past year one of the driest on record in the eastern Horn. [http://www.fews.net/docs/Publications/FEWS NET EA_Historical drought context_061411.pdf](http://www.fews.net/docs/Publications/FEWS_NET_EA_Historical_drought_context_061411.pdf)
- Findlater J (1977) Observational aspects of the low-level cross-equatorial jet stream of the western Indian Ocean. *Monsoon Dynamics*. Birkhäuser Basel, pp 1251–1262
- Funk C (2011) We thought trouble was coming. *Nature* 476(7358):7–7
- Giorgi F, Gutowski WJ (2015) Regional dynamical downscaling and the CORDEX Initiative. *Annu Rev Environ Resour* 40:467–490
- Giorgi F, Jones C, Asrar GR (2009) Addressing climate information needs at the regional level: the CORDEX framework. *WMO Bull* 58:175
- Hargreaves GH, Samani ZA (1985) Reference crop evapotranspiration from temperature. *Appl Eng Agric* 1(2):96–99
- Harris IPDJ, Jones PD, Osborn TJ, Lister DH (2014) Updated high-resolution grids of monthly climatic observations—the CRU TS3. 10 Dataset. *Int J Climatol* 34(3):623–642
- Indeje M, Semazzi FHM (2000) Relationships between QBO in the lower equatorial stratospheric zonal winds and East African seasonal rainfall. *Meteorog Atmos Phys* 73(3):227–244

- IPCC (2014) "Africa" Climate change 2014: Impacts, Adaptation, and Vulnerability. Part B: Regional Aspects. Contribution of Working Group II to the 5th Assessment Rep. of the Intergovernmental Panel on Climate Change. Cambridge University Press, Cambridge, pp 1199–1265
- James R, Washington R (2013) Changes in African temperature and precipitation associated with degrees of global warming. *Clim Chang* 117:859. <https://doi.org/10.1007/s10584-012-0581-7>
- Jolliffe IT (2002) Principal component analysis. John Wiley and Sons, Ltd
- Karmalkar AV, Bradley RS (2017) Consequences of global warming of 1.5 C and 2 C for regional temperature and precipitation changes in the contiguous United States. *PLoS One* 12(1):e0168697
- Kijazi AL, Reason CJC (2009) Analysis of the 1998 to 2005 drought over the northeastern highlands of Tanzania. *Clim Res* 38(3):209–223
- King AD, Karoly DJ, Henley BJ (2017) Australian climate extremes at 1.5°C and 2 °C of global warming. *Nature Climate Change*
- Lott F, Christidis N, Stott PA (2013) Can the 2011 East African drought be attributed to human-induced climate change? *Geophys Res Lett* 40:1177–1181
- Lyon B (2014) Seasonal drought in the Greater Horn of Africa and its recent increase during the March–May long rains. *J Clim* 27(21):7953–7975
- Lyon B, DeWitt DG (2012) A recent and abrupt decline in the East African long rains. *Geophys Res Lett* 39:L02702
- Mavromatis T (2007) Drought index evaluation for assessing future wheat production in Greece. *Int J Climatol* 27(7):911–924
- Monteith JL (1965) Evaporation and environment. *Symposia of the society for experimental biology* (Vol. 19, pp. 205–234). Cambridge University Press (CUP) Cambridge
- Muller JCY (2014) Adapting to climate change and addressing drought–learning from the Red Cross Red Crescent experiences in the Horn of Africa. *Weather Clim Extremes* 3:31–36
- Nguvava M, Abiodun BJ, Otieno F (2019) Projecting drought characteristics over East African basins at specific global warming levels. *Atmos Res* 228:41–54
- Nguvava, M.M., (2020). Understanding the characteristics of droughts over Eastern Africa in past and future climates. Dissertation, University of Cape Town.
- Niang I, Ruppel OC, Abdrabo MA, Essel A, Lennard C, Padgham J, Urquhart P (2014) Africa Climate Change 2014: Impacts, Adaptation, and Vulnerability. Part B: Regional Aspects. Contribution of Working Group II to the Fifth Assessment Report of the Intergovernmental Panel on Climate Change. Cambridge, UK, pp 1199–1265
- Nicholson SE (1996) A review of climate dynamics and climate variability in Eastern Africa. The limnology, climatology and paleoclimatology of the East African lakes. pp 25–56
- Nicholson SE (2017) Climate and climatic variability of rainfall over eastern Africa. *Rev Geophys* 55(3):590–635
- Nikulin G, Lennard C, Dosio A, Kjellström E, Chen Y, Hänsler A, Kupiainen M, Laprise R, Mariotti L, Maule CF, van Meijgaard E (2018) The effects of 1.5 and 2 degrees of global warming on Africa in the CORDEX ensemble. *Environ Res Lett* 13(6):065003
- Omumbo JA, Lyon B, Waweru SM, Connor SJ, Thomson MC (2011) Raised temperatures over the Kericho tea estates: revisiting the climate in the East African highlands malaria debate. *Malar J* 10(1):12
- Osima S, Indasi VS, Zaroug M, Endris HS, Gudoshava M, Misiani HO, Nimusiima A, Anyah RO, Otieno G, Ogwang BA, Jain S (2018) Projected climate over the Greater Horn of Africa under 1.5 C and 2 C global warming. *Environ Res Lett* 13(6):065004
- Otieno VO, Anyah RO (2013) CMIP5 simulated climate conditions of the Greater Horn of Africa (GHA). Part II: projected climate. *Clim Dyn* 41(7–8):2099–2113
- Patricola CM, Cook KH (2011) Sub-Saharan Northern African climate at the end of the twenty-first century: forcing factors and climate change processes. *Clim Dyn* 37(5):1165–1188
- Penman HL (1948) Natural evaporation from open water, bare soil and grass. *Proc Math Phys Eng Sci P Roy Soc A-Math Phys* 193(1032):120–145
- Peters GP, Andrew RM, Boden T, Canadell JG, Ciais P, Le Quééré C, Marland G, Raupach MR, Wilson C (2013) The challenge to keep global warming below 2 C. *Nat Clim Chang* 3(1):4–6
- Philip S, Kew SF, van Oldenborgh GJ, Otto F, O’Keefe S, Haustein K, King A, Zegeye A, Eshetu Z, Hailemariam K, Singh R (2018) Attribution analysis of the Ethiopian drought of 2015. *J Clim* 31(6):2465–2486
- Pinto I, Jack C, Hewitson B (2018) Process-based model evaluation and projections over southern Africa from coordinated regional climate downscaling experiment and coupled model intercomparison project phase 5 models. *Int J Climatol* 38(11):4251–4261
- Richman MB (1986) Rotation of principal components. *Int J Climatol* 6(3):293–335

- Ritchie JT (1983) Efficient water use in crop production: discussion on the generality of relations between biomass production and evapotranspiration. Limitations to efficient water use in crop production, (limitationstoef). pp 29–44
- Robinson C, Zimmerman L, Checchi F (2014) Internal and external displacement among populations of Southern and Central Somalia Affected by Severe Food Insecurity and Famine during 2010–2012. FEWS NET, Washington, DC, USA
- Rummukainen M (2010) State-of-the-art with regional climate models. *Wiley Interdiscip Rev Clim Chang* 1(1):82–96
- Santos JF, Pulido-Calvo I, Portela MM (2010) Spatial and temporal variability of droughts in Portugal. *Water Resour Res* 46: W03503
- Segele ZT, Lamb PJ, Leslie LM (2009) Seasonal-to-interannual variability of Ethiopia/horn of Africa monsoon. Part I: associations of wavelet-filtered large-scale atmospheric circulation and global sea surface temperature. *J Clim* 22(12):3396–3421
- Shongwe ME, van Oldenborgh GJ, van den Hurk B, van Aalst M (2011) Projected changes in mean and extreme precipitation in Africa under global warming. Part II: East Africa. *J Clim* 24(14):3718–3733
- Souverein N, Thiery W, Demuzere M, Van Lipzig NPM (2016) Drivers of future changes in East African precipitation. *Environ Res Lett* 11(11):114011
- Stevenson S, Fox-Kemper B, Jochum M, Neale R, Deser C, Meehl G (2011) Will there be a significant change to El Niño in the twenty-first century? *J Clim* 25(6):2129–2145
- Su B, Jian D, Li X, Wang Y, Wang A, Wen S, Tao H, Hartmann H (2017) Projection of actual evapotranspiration using the COSMO-CLM regional climate model under global warming scenarios of 1.5° C and 2.0° C in the Tarim River Basin, China. *Atmos Res* 196:119–28
- Thornthwaite CW (1948) An approach toward a rational classification of climate. *Geogr Rev* 38(1):55–94
- Tierney JE, Smerdon JE, Anchukaitis KJ, Seager R (2013) Multidecadal variability in East African hydroclimate controlled by the Indian Ocean. *Nature* 493(7432):389–392
- Trenberth KE, Dai A, Van Der Schrier G, Jones PD, Barichivich J, Briffa KR, Sheffield J (2014) Global warming and changes in drought. *Nat Clim Chang* 4(1):17–22
- Ujeneza EL, Abiodun BJ (2015) Drought regimes in Southern Africa and how well GCMs simulate them. *Clim Dyn* 44(5–6):1595–1609
- UNDP (2008) Climate change and human development in Africa: assessing the risks and vulnerability of climate change in Kenya, Malawi and Ethiopia. Human Development Report 2007-08. United Nations Development Programme (UNDP), Intergovernmental Authority on Development and the Climate Prediction and Applications Centre
- UNFCCC (2015) Report on the Structured Expert Dialogue (SED) on the 2013–2015 Review. FCCC/SB/2015/INF.1
- Vautard R, Gobiet A, Sobolowski S, Kjellstrom E, Stegehuis A, Watkiss P, Mendlik T, Landgren O, Nikulin G, Teichmann C, Jacob D (2014) The European climate under a 2oC global warming. *Environ Res Lett* 9:034006
- Vecchi GA, Wittenberg AT (2010) El Niño and our future climate: where do we stand? *Wiley Interdiscip Rev Clim Chang* 1(2):260–270
- Vicente-Serrano SM, Beguería S, Gimeno L, Eklundh L, Giuliani G, Weston D, El Kenawy A, López-Moreno JI, Nieto R, Ayenew T, Konte D (2012) Challenges for drought mitigation in Africa: the potential use of geospatial data and drought information systems. *Appl Geogr* 34:471–486
- Vicente-Serrano SM, Beguería S, López-Moreno JI (2010) A multiscalar drought index sensitive to global warming: the standardized precipitation evapotranspiration index. *J Clim* 23(7):1696–1718
- Viste E, Korecha D, Sorteberg A (2013) Recent drought and precipitation tendencies in Ethiopia. *Theor Appl Climatol* 112(3–4):535–551
- Vizy EK, Cook KH (2003) Connections between the summer east African and Indian rainfall regimes. *J Geophys Res-Atmos* 108(D16):4510
- Wang G, Cai W, Gan B, Wu L, Santoso A, Lin X, Chen Z, McPhaden MJ (2017) Continued increase of extreme El Niño frequency long after 1.5° C warming stabilization. *Nature. Climate Change* 7(8):568–572
- Yang W, Seager R, Cane MA, Lyon B (2015) The annual cycle of East African precipitation. *J Clim* 28(6):2385–2404
- Ying X, Bo-Tao Z, Jie W, Zhen-Yu H, Yong-Xiang Z, Jia W (2017) Asian climate change under 1.5–4° C warming targets. *Adv Clim Chang Res* 8(2):99–107